Photodisintegration of light nuclei for testing a correlated realistic interaction in the continuum

Sonia Bacca*
Gesellschaft für Schwerionenforschung, Planckstr. 1, 64291 Darmstadt, Germany
(Dated: February 8, 2008)

An exact calculation of the photodisintegration cross section of ^{3}H, ^{3}He and ^{4}He is performed using as interaction the correlated Argonne V18 potential, constructed within the Unitary Correlation Operator Method ($V_{\rm UCOM}$). Calculations are carried out using the Lorentz Integral Transform method in conjunction with an hyperspherical harmonics basis expansion. A comparison with other realistic potentials and with available experimental data is discussed. The $V_{\rm UCOM}$ potential leads to a very similar description of the cross section as the Argonne V18 interaction with the inclusion of the Urbana IX three-body force for photon energies $45 \leq \omega \leq 120$ MeV, while larger differences are found close to threshold.

PACS numbers: 21.45.+v, 21.30.-x, 25.20.Dc, 27.10.+h

I. INTRODUCTION

One of the main challenges in theoretical nuclear physics is a microscopic description of the properties of finite nuclei, using realistic nuclear forces. For a given interaction model, appropriate observables showing impact on different features of the nuclear potential need to be tested in a many-body system through direct comparison with experimental data. In few-particle systems, where the quantum many-body problem of nucleons can be solved exactly both for bound and scattering states, one has an optimal setting to probe off-shell properties of different potentials.

For photodisintegration of light nuclei, exact calculations predict a slightly different behavior when using different two-body realistic interactions, while a more evident effect of three-body forces is found. However, the experimental situation is still unsatisfactory, as the data are not sufficiently precise to discriminate clearly among different interactions models. Among light nuclei, the photoexcitation of the alpha particle has recently attracted much attention both in theory, where a calculation with realistic two- and three-body forces was carried out [1], and in experiments [2, 3], where the aim was to further clarify whether ^{4}He exhibits a pronounced giant dipole resonance or not, a question that was raised in the first microscopic calculation of the reaction [4], where semirealistic two-body forces where used. Unfortunately, experimental data do not yet lead to a unique picture. Nevertheless, a comparison of the impact on observables of different potentials on a theoretical level is already instructive.

These exact calculations of the photodisintegration cross section can also offer valuable theoretical guidance in a class of astrophysical studies. Nuclear absorption of high-energy γ-rays through excitations of giant resonances may potentially become an important diagnostic tool for the dense environments of compact astrophysical sources. For example, black holes emit an intense high-energy γ-ray continuum, against which nuclear absorption features would uniquely probe the baryonic-matter density, and possibly some compositional information, near the source. Since the dependency on the potential model used in our calculations turns out to be small in comparison to the discrepancy in experiments, our precise microscopic reaction calculations can help to investigate interstellar gas, mostly isotopes of hydrogen and helium, surrounding the astrophysical γ-ray source [5].

The purpose of this paper is to investigate the total photodisintegration cross section of light nuclei using the potential constructed within the Unitary Correlation Method (UCOM), denoted with $V_{\rm UCOM}$. This is aimed at testing for the first time this interaction in a continuum reaction, where many disintegration channels are open, and simultaneously studying the capability of describing electromagnetic reactions via non-local two-body interactions *versus* local two-and three-body models. Exact calculations are performed making use of the Lorentz Integral Transform (LIT) approach [6], which enables to fully take into account the final state interaction, while circumventing the difficulties arising from the continuum many-body scattering states. The problem is in fact reduced to the solution of a bound-state-like equation, which we solve with an hyperspherical harmonics (HH) basis.

The paper is organized as follows. In Sec. II the theoretical background is set: an overview of the UCOM is given, then the LIT method is briefly summarized. In Sec. III results are shown and conclusions are finally drawn in Sec. IV.

II. THEORETICAL OVERVIEW

A. The Unitary Correlation Operator Method

Different models for the nucleon-nucleon (NN) interaction are found in the literature, as *e.g.* the Argonne V18

*electronic address: s.bacca@gsi.de

potential (AV18) [7], the CD Bonn [8] and the Nijmegen [9] potentials. These modern two-body interactions reproduce the experimental NN data with high precision, but they underbind nuclei with $A \geq 3$. This drawback has traditionally been overcome introducing phenomenological three-body forces fitted to reproduce experimental binding energies and first excited states of light nuclei. Furthermore, chiral perturbation theory can provide a systematic way to build two-, three- and more-body forces [10, 11]. The above mentioned potential models, including two- and three-body forces have been used to calculate bound state properties of light nuclei (up to $A = 12$ and more), mainly within the Green's function Monte Carlo (GFMC) method [12, 13, 14] and the no-core shell model (NCSM) approach [15, 16, 17]. However, the addition of a three nucleon potential requires a very intensive computational effort when used in many-body systems. In Ref. [18] it was shown that different, but phase equivalent two-body interactions are related by a unitary non-local transformation. It is expected that the addition of non-locality to the NN interaction could reduce or even cancel the need of three-body force, leading to a big simplification of many-body calculations. Based on this idea, a new category of NN potentials has then emerged, among them one can recall: (i) the Inside Nonlocal Outside Yukawa (INOY) interaction by Doleshall *et al.* [19], (ii) the J-matrix Inverse Scattering Potential (JISP) by Shirokov *et al.* [20, 21] and (iii) the Unitary Correlation Operator Method (UCOM) by Feldmeier *et al.* [22, 23, 24]. The $V_{\rm UCOM}$ potential derived from the AV18 interaction has already been used as universal input in quite a variety of many-body techniques, ranging form Hartree-Fock calculations [25], to Random Phase Approximation [26] and to nuclear structure calculations in the framework of Fermionic Molecular Dynamics, see *e.g.* [27, 28].

In the UCOM framework the dominant short range-correlations, induced by the repulsive core and by the tensor part of the NN interaction, are explicitly described by a state independent unitary transformation. When the correlation operator is applied to the Hamiltonian, a phase-shift equivalent correlated interaction is obtained. A correlated operator is defined via a similarity transformation

$$\tilde{O} = \hat{C}_\Omega^{-1}\hat{C}_r^{-1}\hat{O}\hat{C}_r\hat{C}_\Omega\,, \tag{1}$$

where $\hat{C}_r$ and $\hat{C}_\Omega$ are the unitary radial and tensor correlation operators, respectively. The correlator $\hat{C}_r$ introduces a radial distance-dependent shift which keeps nucleons away from each other when their uncorrelated distance is smaller than the range of the strongly repulsive core of the NN interaction. $\hat{C}_\Omega$ produces tensor correlations by further spatial shifts perpendicular to the radial direction, depending on the orientation of the spins of the two nucleons with respect to their distance.

In a many-body system the correlated operator of Eq. (1) becomes an A-body operator with irreducible n-body contributions, $n = 1, \ldots, A$,

$$\tilde{O} = \tilde{O}^{[1]} + \tilde{O}^{[2]} + \tilde{O}^{[3]} + \ldots \tilde{O}^{[A]}\,, \tag{2}$$

where $\tilde{O}^{[n]}$ indicates the irreducible n-body part. In the UCOM one usually employs a two-body cluster approximation, neglecting $\tilde{O}^{[3]}$ and higher cluster orders. The effect of this approximation was tested in the framework of NCSM, where one can perform exact few-body calculations [29]. In particular, in this reference it was shown that the omitted three- and more-body terms of the cluster expansion can be tuned changing the range of the tensor correlators in order to compensate the genuine three-body force to a large extent, still preserving the phase shift equivalence. The value of the tensor "correlation volume" $I_\theta^{(1,0)} = 0.09$ fm^3 (for details see [29]) was found to give the best description of binding energies of ^{3}H and ^{4}He on the Tjon line. In this paper we will use this very same value of $I_\theta^{(1,0)}$ in order to investigate whether the non-local two-body $V_{\rm UCOM}$ interaction, that minimizes the effect of three-body forces on the binding energies, can also describe the continuum photoabsorption cross section.

As already pointed out in [18], phenomenological non-local interaction terms introduce modifications on the electromagnetic current operator, conserved by gauge invariance. In fact, if the nuclear potential V does not commute with the charge operator, then two-body currents, usually called Meson Exchange Currents (MEC), have to be introduced, for consistency. In case of phenomenological non-local potentials the explicit construction of a consistent MEC could be rather involved. The study of electromagnetic reactions at low energies, where one can use the Siegert theorem (see *e.g.* [30]), allows to investigate the role of implicit electromagnetic exchange mechanisms without requiring an explicit knowledge of the two-body current operator. For this reason, the test of a given potential model on the prediction for photoabsorption cross section is very important.

B. The Lorentz Integral Transform approach

The total photoabsorption cross section is given by

$$\sigma(\omega) = 4\pi^2\alpha\omega R(\omega)\,, \tag{3}$$

where α is the electromagnetic coupling constant and, at low photon energy ω, $R(\omega)$ is the inclusive unpolarized dipole response function, generally defined as:

$$R(\omega) = \frac{1}{2J_0+1}\sum_{M_0}\sum_f \left|\langle\Psi_f|\,\hat{D}_z\,|\Psi_0\rangle\right|^2 \delta(E_f - E_0 - \omega)\,. \tag{4}$$

Here, J_0 and M_0 indicate the total angular momentum of the nucleus in its initial ground state and its projection, while $\left|\Psi_{0/f}\right\rangle$ and $E_{0/f}$ denote wave function and energies of the ground and final states, respectively. The dipole

operator is

$$\hat{D}_z = \frac{1}{2}\sum_i \hat{z}_i \hat{\tau}_i^3 \,, \tag{5}$$

where $\hat{z}_i$ and $\hat{\tau}_i^3$ are the third components of the position in the center of mass reference frame and isospin of the i-th particle, respectively. The dipole approximation has been proven to be very good at low photon energy for the deuteron [31] and for the triton case [32]. With the dipole operator the major part of the meson exchange currents (MEC) is implicitly taken into account, via the Siegert theorem.

In the LIT method [6] one obtains $R(\omega)$ after the inversion of an integral transform with a Lorentzian kernel

$$L(\sigma_R,\sigma_I) = \int d\omega \frac{R(\omega)}{(\omega-\sigma_R)^2+\sigma_I^2} = \langle\widetilde{\Psi}|\widetilde{\Psi}\rangle \,, \tag{6}$$

where $|\widetilde{\Psi}\rangle$ is the unique solution of the inhomogeneous "Schrödinger-like" equation

$$(\hat{H}-E_0-\sigma_R+i\sigma_I)|\widetilde{\Psi}\rangle = \hat{D}_z|\Psi_0\rangle. \tag{7}$$

Because of the presence of an imaginary part σ_I in Eq. (7) and the fact that the right-hand side of this equation is a localized state, one has an asymptotic boundary condition similar to a bound state. Thus, one can apply bound-state techniques for its solution. The response function $R(\omega)$ is recovered via an inversion of the integral transform of Eq.(6) (for inversion methods see Refs. [33] and [34]). Up to now this method has allowed calculations of electromagnetic reactions for ^{3}H and ^{3}He [32, 35, 36, 37] and recently even for ^{4}He [1] with realistic two- and three-body forces. Nuclei with six- [38, 39] and even seven nucleons [40] have been investigated with semirealistic interactions. A similar formalism has been applied to describe exclusive electromagnetic processes in the four-body system with semirealistic potentials [41, 42, 43]. Recently, the method has been also applied to the harmonic oscillator basis in the framework of NCSM [44].

In the present paper we calculate the LIT using an HH expansion of the internal wave function. For the antisymmetrization of the wave function we make use of the powerful algorithm developed by Barnea *et al.* [45, 46, 47]. The HH approach, which is natural in coordinate space for a local interaction, has been recently extended to the use of non-local potentials given in terms of two-body matrix elements between harmonic oscillator (HO) states [48], like the JISP potential. In this paper we will make use of the same method using as input the correlated HO matrix elements of the AV18 potential, constructed within the UCOM.

III. RESULTS

We begin the discussion with the results for the ground state energies of ^{4}He and ^{3}H calculated in the HH expansion with $V_{\rm UCOM}$. Even if the starting point is the local

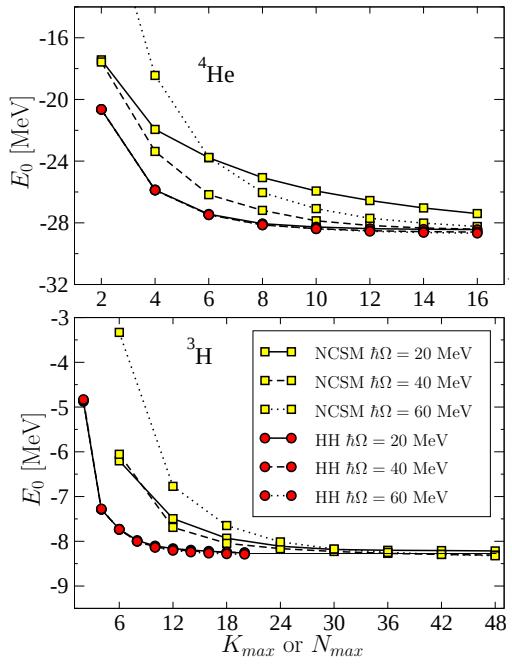

FIG. 1: (Color online) Ground-state energies of ^{4}He and ^{3}H with the $V_{\rm UCOM}$ potential for different values of the HO parameter $\hbar\Omega$ as a function of the HO excitations N_{max} allowed in the NCSM model space and of the maximal value of the HH grand-angular momentum quantum number K_{max} in the HH expansion ($n_{max}=15$).

AV18 potential, the correlated $V_{\rm UCOM}$ contains derivative operators. In principle, one could extend the HH formalism to the use of such terms and consider the rather involved operator form of the $V_{\rm UCOM}$, the result being a more intensive numerical computation for each matrix element. The alternative approach we use, consists in representing the two-body potential operator on an HO basis, similarly to the case of the JISP potential. The input of our HH calculation are the correlated relative two-body HO matrix elements,

$$v^{jm,\hbar\Omega}_{nn'\ell\ell'ss'} = \langle n(\ell s)jm|\tilde{v}_{\rm UCOM}|n'(\ell's')jm\rangle\big|_{\hbar\Omega} \,, \tag{8}$$

where n,ℓ, s and j are radial quantum number, orbital angular momentum, spin and total angular momentum of the two-body sub-system, respectively (isospin is omitted for the sake of simplicity). In the operator form the UCOM is independent on the HO parameters, therefore the HO representation should be viewed as a parameterization rather than a formulation of the potential. In fact, we expand the two-body potential as

$$\hat{V} = \sum_{nn'}^{n_{max}} \sum_{\ell\ell'}^{\ell_{max}} \sum_{jmss'} |n(\ell s)jm\rangle v^{jm,\hbar\Omega}_{nn'\ell\ell'ss'} \langle n'(\ell's')jm| \,. \tag{9}$$

The sum over two-body quantum numbers n, n' and ℓ, ℓ' has to be performed up to maximal value of n_{max} and

TABLE I: Ground state energies in MeV with the $V_{\rm UCOM}$ potential. NCSM results from [29]. HH calculations performed with n_{max}=15.

Method	^{4}He	^{3}H
NCSM	-28.4(1)	-8.32(3)
HH	-28.57(3)	-8.27(2)
Nature	-28.30	-8.48

ℓ_{max} for the radial quantum number and angular momentum, respectively. The expansion has to be pushed forward, till independence of observables, like binding energies, on the HO parameters is reached. We find out that good convergence of the angular part is reached with $\ell_{max} = 6$, while at least $n_{max} = 15$ oscillator quanta are needed for the radial part.

Since we work in an hyperspherical harmonics many-body Hilbert space, convergence as a function of the hyperspherical grand angular momentum K_{max} needs to be further investigated. In Fig. 1, we compare the HH results *versus* K_{max} with the NCSM data from [29] as a function of the HO excitation allowed $N_{max} = \sum_i 2n_i + \ell_i$, where i runs over the $A-1$ Jacobi coordinates. Results for different values of the HO parameter $\hbar\Omega$ are presented. As one can note, the NCSM $\hbar\Omega$-dependence is rather strong, while the HH approach is almost HO parameter free. The small residual $\hbar\Omega$-dependence, of the order of 0.7%, is due to the truncation in Eq. (9). The HH convergence as a function of K_{max} is much faster than the NCSM convergence in N_{max}. This is strongly manifested in case of the more extended nucleus of ^{3}H, where convergence of the NCSM is reached only with $N_{max} = 48$. The reason for that lies in the fact that in the HH-approach matrix elements with oscillator quanta up to $n_{max} = 15$ of the two-body subsystem are considered for each K_{max} value, and not only beyond $N_{max} = 30$, as for the NCSM. In Table I the result for ground state energies of $V_{\rm UCOM}$ for ^{4}He and ^{3}H are summarized. The NCSM results correspond to the $\hbar\Omega$ that yields the minimal energy for the largest model space used, whereas for the HH results the mean value of the different $\hbar\Omega$ has been taken. The two methods agree with each other. The slightly lower ^{4}He and the slightly higher ^{3}H binding energies in HH are related to the different Hilbert spaces. They are consistent with the fact that in the HH-approach with $\ell_{max} = 6$ and $n_{max} = 15$ one takes into account higher two-body HO excitations than with $N_{max} = 16$, but less than with $N_{max} = 48$.

The ground state wave function $|\Psi_0\rangle$ and energy E_0 are then used in Eq. (7) to address the problem of the continuum with the LIT method. In Fig. 2, we show the transforms $L(\sigma_R, \sigma_I = 20$ MeV) in case of ^{4}He as a function of the parameter σ_R for $\hbar\Omega$ fixed to 20 MeV. The convergence in terms of the HH expansion is studied as a function of the K_{max}: the even/odd value of K_{max} is due to parity difference of the expanded states, $|\Psi_0\rangle$ and

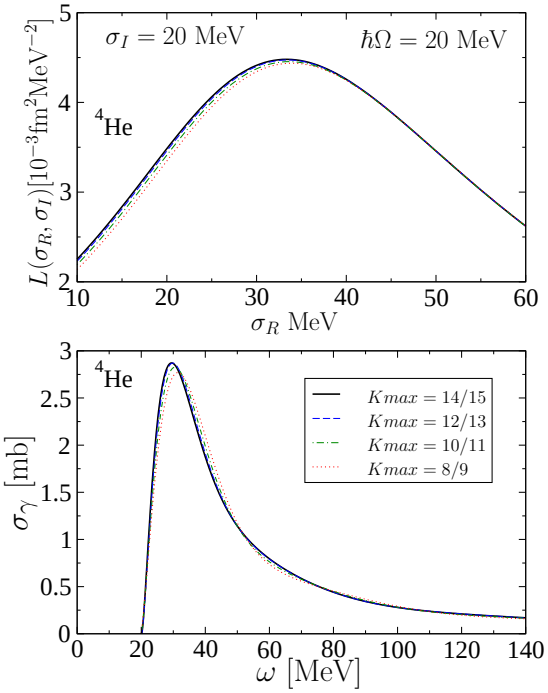

FIG. 2: (Color online) ^{4}He: (upper panel) convergence of the LIT, with fixed $\sigma_I = 20$ MeV and HO parameter $\hbar\Omega = 20$ MeV, for different values of the hyperspherical grand-angular momentum quantum number K_{max} in the HH expansion ($n_{max} = 15$); (lower panel) convergence of the photoabsorption cross section.

$\hat{D}|\Psi_0\rangle$, respectively. After inverting the various transform and making use of Eq. (3) one can observe the convergence of the photoabsorption cross section. Full convergence is reached with $K_{max} = 14/15$ both for the LIT and for σ_γ. Similar behavior in K_{max}, though slightly weaker, is obtained for the $\hbar\Omega$ values of 40 and 60 MeV. In an analogous way we have investigated the ^{3}H case, where full convergence is reached with $K_{max} = 16/17$. The broader structure of ^{3}H with respect to ^{4}He makes the rate of convergence slightly slower.

At this point it is convenient to compare the converged cross sections obtained with different HO parameters to investigate the $\hbar\Omega$ dependence in the continuum. As one can see in Fig. 3 in case of ^{4}He one gets stable results for σ_γ with $n_{max} = 15$. The residual $\hbar\Omega$ dependence can be interpreted as the numerical error of our calculations: the indetermination is maximally 1.5% in the dipole resonance peak region and never exceeds 6% for higher energies. On the contrary, in case of ^{3}H the HO parameter dependence is still rather strong with $n_{max} = 15$, thus higher values of n_{max} need to be considered in the expansion of Eq. (9). In particular, we observed that for the larger $\hbar\Omega = 40$ and 60 MeV values, higher n_{max} are needed to obtain stable result for the cross section. To check the degree of convergence in the continuum one can investigate the first sum rules of the cross section. For example, we have considered the inverse energy-weighted

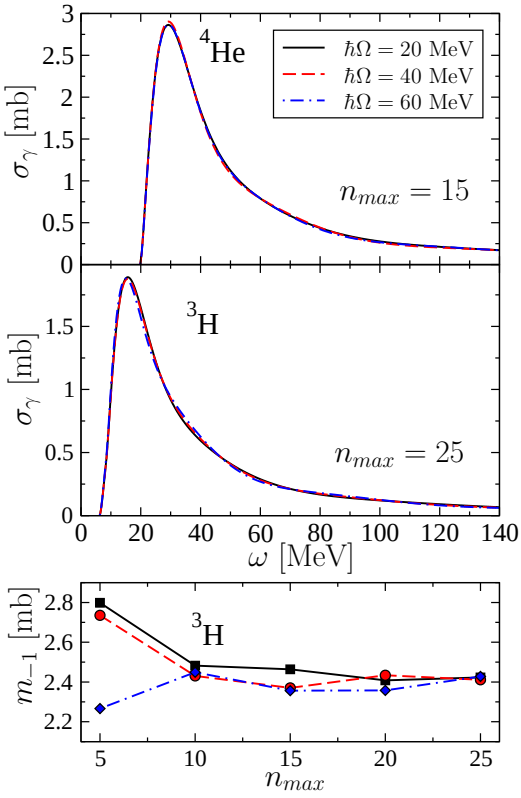

FIG. 3: (Color online) Photoabsorption cross section of ^{4}He (upper panel) and ^{3}H (middle panel) for different values of the HO parameter $\hbar\Omega$. For ^{4}He a maximal value $n_{max} = 15$ in the correlated HO matrix element is used in input, while for ^{3}H $n_{max} = 25$ is considered. (Lower panel) convergence of the sum rule m_{-1} for ^{3}H as a function of n_{max}.

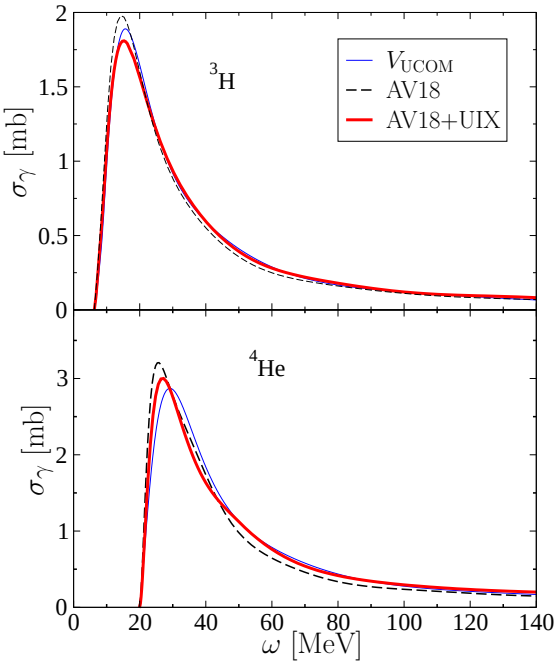

FIG. 4: (Color online) Photodisintegration cross section of triton (upper panel) and ^{4}He (lower panel) with different potential models: (thin line) $V_{\rm UCOM}$, (dashed line) bare AV18 and (thick line) AV18+UIX force.

sum rule of the cross section m_{-1} (proportional to the total dipole strength), evaluated as expectation value on the ground state [49],

$$m_{-1} = \int_{\omega_{th}}^{\infty} \frac{\sigma_\gamma(\omega)}{\omega}\, d\omega = \frac{4\pi^2\alpha}{3}\left[Z^2\,\langle r_p^2\rangle - \frac{Z(Z-1)}{2}\,\langle r_{pp}^2\rangle\right]. \quad (10)$$

Here $\langle r_p^2\rangle$ and $\langle r_{pp}^2\rangle$ are the mean square point-proton and mean square proton-proton radii. In Fig. 3, the behavior of the m_{-1} for ^{3}H as a function of n_{max} (for converged expansion in K_{max}) is shown for different HO frequencies. One can see that for $n_{max} = 15$ the discrepancy is of about 5% ($1 - 2\%$ in case of ^{4}He), while only with $n_{max} = 25$ a satisfactory $\hbar\Omega$-independence (0.5%) is achieved. This is again due to the fact that the ^{3}H wave function has a longer range structure than ^{4}He, thus convergence is slower. Furthermore, the higher sensitivity of m_{-1} in n_{max} with respect to E_0 (^{3}H binding energies decreases of only 30 KeV going from $n_{max} = 15$ to 25) is related to the long range nature of the operator. In the peak region, the final ^{3}H photoabsorption cross section presents a 1% difference between the $\hbar\Omega = 20$ MeV and the $\hbar\Omega = 40$ MeV results, and about 4% between the $\hbar\Omega = 20$ MeV and the $\hbar\Omega = 60$ MeV. The reason of the poorer convergence for a high HO parameter in the continuum was already pointed out in [44], where the LIT method was applied for the first time to the NCSM basis. Here, though we use an HH basis, the parameterization of the potential via HO two-body matrix element leaves some fingerprints, *i.e.* a slight residual $\hbar\Omega$ dependence. As the HO potential well becomes steeper and steeper, the two-body wave functions in a fixed model space (fixed n_{max}) go faster to zero, consequence being a poorer representation of long-range operators, like the dipole. Thus, higher n_{max} need to be considered to get the same degree of of accuracy. On the contrary, for smaller HO frequencies, the two-body HO eigenstates are closer to each other, resulting in a better sampling of the complex-energy continuum of the LIT, and thus in a better convergence of the cross section.

In Fig. 4, we compare the photoabsorption cross section with $V_{\rm UCOM}$ to those obtained with other potential models: the AV18 potential and the AV18 with the inclusion of the Urbana IX three-body force, AV18+UIX. Predictions for ^{3}H and ^{4}He are taken from [32] and [1], respectively. The addition of the short range non-locality introduced by the correlators in the UCOM has consequences on σ_γ. In fact, with respect to the usual AV18 potential, the $V_{\rm UCOM}$ leads to a reduction of the peak cross section of about 4% for ^{3}H and 10% for ^{4}He, while a general enhancement of the tail of the cross section is found: it amounts, for example, to 15% and 23% at $\omega = 60$ MeV, for ^{3}H and ^{4}He, respectively. Similar effects

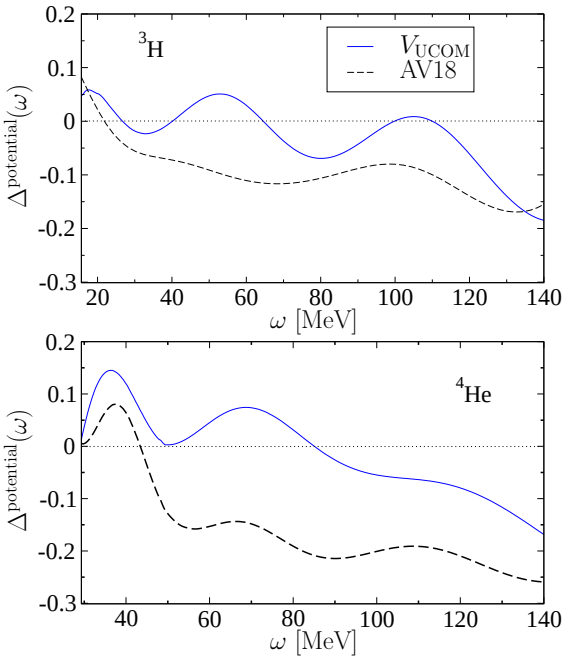

FIG. 5: (Color online) Quantity $\Delta^{\rm potential}(\omega)$ (see text) as a function of the photon energy in case of ^{3}H and ^{4}He for the $V_{\rm UCOM}$ and AV18 potentials.

on the photoabsorption cross section are obtained with the introduction of the UIX three-body force, though with some differences. With respect to the interaction model of AV18+UIX the $V_{\rm UCOM}$ potential leads to a 4% higher photodisintegration peak in case of ^{3}H and to a 4% lower one for ^{4}He. We also observe a 0.5 and 2 MeV shift of the peak position towards higher energies for ^{3}H and ^{4}He, respectively. At low photon energies prediction of $V_{\rm UCOM}$ are lower than AV18+UIX: for example the difference is about 10% for ^{3}H and 25% for ^{4}He at 3.5 MeV after disintegration threshold. Interestingly, the tail of the photoabsorption cross section obtained with the $V_{\rm UCOM}$ is very similar (less than $6-7$% difference) to the AV18+UIX result for photon energy $20 \leq \omega \leq 120$ MeV in case of ^{3}H and $45 \leq \omega \leq 100$ MeV for the alpha particle.

We observe that with the $V_{\rm UCOM}$ a reduction of the missing genuine three-body force is achieved for high photon energies. In fact, keeping as reference the AV18+UIX curve, the relative difference on σ_γ, defined as

$$\Delta^{\rm potential}(\omega) = \left[1 - \frac{\sigma_\gamma^{\rm potential}(\omega)}{\sigma_\gamma^{\rm AV18+UIX}(\omega)}\right] \qquad (11)$$

gives information on that. In Fig. 5, the quantity $\Delta^{\rm potential}(\omega)$ is presented in case of ^{3}H and ^{4}He for ω beyond the corresponding peak energies obtained with $V_{\rm UCOM}$. In case of ^{3}H, $\Delta^{\rm potential}(\omega)$ is reduced by at least a factor 2 in the energy region $25 \leq \omega \leq 75$ MeV and $90 \leq \omega \leq 120$, going from the AV18 to the $V_{\rm UCOM}$ potential. An even stronger reduction effect is found for ^{4}He for energies between 45 MeV and pion threshold.

Potential	$\langle r_p^2 \rangle$ ^{3}H	$\langle r^2 \rangle$ ^{4}He	$\langle r_{pp}^2 \rangle$ ^{4}He
$V_{\rm UCOM}$	2.52(1)	1.96(1)	5.41(1)
AV18+UIX	2.51(1)	2.05(1)	5.67(1)

TABLE II: Mean square point proton and proton-proton radii in fm^2 with $V_{\rm UCOM}$ and AV18+UIX ($\langle r_p^2 \rangle = \langle r^2 \rangle$ for ^{4}He without isospin-mixing). Results for triton from [50] and for alpha particle from [51].

In the following an investigation of two photonuclear sum rules, the already mentioned m_{-1} (Eq. (10)) and the Thomas-Reiche-Kuhn (TRK) sum rule [52]

$$m_0 = \int_{\omega_{th}}^{\infty} \sigma_\gamma(\omega)\, d\omega \qquad (12)$$
$$= \frac{4\pi^2\alpha}{2J_0+1} \sum_{M_0} \left\langle \Psi_0; M_0 | [\hat{D}_z, [\hat{H}, \hat{D}_z]] | \Psi_0; M_0 \right\rangle ,$$

is briefly presented (see also Ref. [51]). With respect to the AV18+UIX case, the $V_{\rm UCOM}$ potential predicts a very similar m_{-1} for ^{3}H and a lower m_{-1} for ^{4}He. This fact is also reflected in the size of the radii of Eq.(10). In Table II we summarize the situation: for ^{3}H we present only the proton radius, since the there is no proton-proton radius, while for ^{4}He we show the squared mass radius ($\langle r^2 \rangle = \langle r_p^2 \rangle$ if isospin mixing is neglected) and $\langle r_{pp}^2 \rangle$. One can see that $V_{\rm UCOM}$ leads almost to the same proton radius as AV18+UIX within a 0.4% deviation, but smaller radii for the alpha particle are obtained, if compared to AV18+UIX. A consequence of that is the lower ^{4}He peak cross section found with $V_{\rm UCOM}$ with respect to AV18+UIX. The TRK sum rule is of interest since it contains information on the exchange mechanisms induced by the non-commuting part of the potential $\hat{V}$. For example, for ^{4}He, we find that $m_0 = 117.6$ mb MeV for $V_{\rm UCOM}$, which is about 20% lower in comparison to the value of 146.2 mb MeV found for AV18+UIX [51]. This is more strongly connected to the fact that with $V_{\rm UCOM}$ the cross section goes faster to zero beyond pion threshold and indicates that the meson exchanges underlying the two potential models are different.

We now compare the theoretical predictions with the available experimental data. Among the theoretical curves we add the result with the JISP potential [21], recently published in [48]. In Fig. 6, we show the situation for the ^{3}He nucleus and for ^{4}He. In case of the three-body nucleus the error bars of the data from Fetisov *et al.* [53] are unfortunately too big to allow us to discriminate among the different potential models.

In case of the alpha particle the experimental situation is more involved. Close to threshold several data were taken in different experiments, which unfortunately show fairly large discrepancies. Only the data from Arkatov *et al.* [54] cover a larger energy range. They present

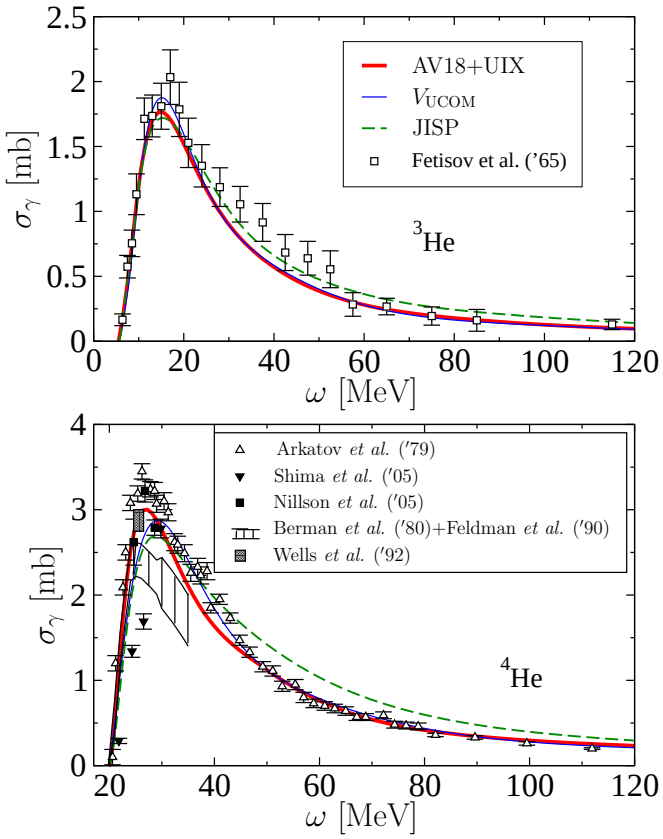

FIG. 6: (Color online) Theoretical photoabsorption cross section of ^{3}He and ^{4}He with three different potential models, (thin line) $V_{\rm UCOM}$, (thick line) AV18+UIX and (dashed line) JISP potential from [48], in comparison with the available experimental data: empty squares from [53] for ^{3}He, empty triangles from [54], full triangles from [3], full squares from [2], shaded area sum of data from [55] and [56] and box from [57] for ^{4}He.

a rather high peak cross section, in fair agreement with recent data from [2], which favors the AV18+UIX potential model. In the energy region $30 \leq \omega \leq 45$ MeV the results with $V_{\rm UCOM}$ agree better with this set of data than those with AV18+UIX. Finally, at higher energies the measurements are precise enough to conclude that AV18+UIX and $V_{\rm UCOM}$ can explain, within the error bars, the photoabsorption cross section, in contradistinction to the JISP potential. In Ref. [48] it was argued that a possible reason of this discrepancy of the JISP model could be due to the probably incorrect long range part of the potential, whose construction is not constrained by the meson exchange theory. Regarding this issue we can only state that $V_{\rm UCOM}$, which explicitly contains the long-range pion exchange term of AV18, unchanged by the short range action of the correlations, exhibits a correct tail behavior in the photoabsorption cross section of light nuclei. Here we would also like to point out that the consideration of large Hilbert spaces (large K_{max} and n_{max}) is essential to achieve a stable and HO-independent result on the whole photon energy range. The fact that the JISP potential is constructed on a small HO basis, for defined n_{max} and $\hbar\Omega$ values, could limit the correct description of the tail of this sensitive observable.

IV. CONCLUSIONS

We have presented the results of an *ab initio* calculation of the ^{3}H, ^{3}He and ^{4}He photodisintegration cross section with the $V_{\rm UCOM}$ potential. The difficulty of the scattering continuum problem is circumvented via the Lorentz Integral Transform method, where the final state interaction is fully taken into account. An expansion of the wave function on hyperspherical harmonics, extended for non-local interaction, is used for the solution of the "Schrödinger-like" equation. The first investigation of the Unitary Correlation Operator Method on a continuum observable is presented in this paper. The sensitivity of the photoabsorption cross section on non-local terms of the interaction is investigated. With respect to the traditional local AV18 potential, a reduction of the peak and an enhancement of the tail of the cross section is produced by the non-locality of $V_{\rm UCOM}$. The comparison between the AV18+UIX potential model and $V_{\rm UCOM}$ allows to investigate, whether the omission of a genuine three-body force can be replaced by a non-local interaction on a continuum observable. Though binding energies of very light nuclei are well described by $V_{\rm UCOM}$ with a $1-2\%$ difference with respect to the AV18+UIX model, the situation is different in the photodisintegration cross section below pion threshold. Our analysis shows that the $V_{\rm UCOM}$ potential leads to a very similar result as the AV18+UIX for high photon energy, while in the region close to threshold larger differences are found, particularly in case of ^{4}He. The larger deviation in ^{4}He with respect to the ^{3}H case could be related to the fact that smaller mean square radii are obtained with the $V_{\rm UCOM}$. The higher density of the alpha particle makes it certainly more sensitive to characteristic short range properties of the three-body force and non-local parts of the NN interaction, magnifying the differences. The similarity of the high-energy cross section shows that also in the continuum genuine three-body forces can be partly simulated with the non-local $V_{\rm UCOM}$ potential. But the differences found at low-photon energies point out that the two potential models are not completely equivalent. Unfortunately, the lack of precise experimental data limits the possibility to use such calculations as a discriminant test of the potentials.

Acknowledgments

The author would like to thank Nir Barnea for providing the HH code extended for the use of non-local in-

teraction, and Robert Roth for supplying the correlated harmonic oscillator matrix element of $V_{\rm UCOM}$. Further gratefulness is owed to Hans Feldmeier, Winfried Leidemann and Giuseppina Orlandini for many useful discussions and for a critical reading of the manuscript. Numerical calculations are partly performed at CINECA (Bologna).

[1] D. Gazit, S. Bacca, N. Barnea, W. Leidemann, and G. Orlandini, Phys. Rev. Lett. **96**, 112301 (2006).
[2] B. Nilsson, J.-O. Adler, B.-E. Andersson, J. R. M. Annand, I. Akkurt, M. J. Boland, G. I. Crawford, K. G. Fissum, K. Hansen, P. D. Harty *et al.*, Phys. Lett. B **626**, 65 (2005).
[3] T. Shima, S. Naito, Y. Nagai, T. Baba, K. Tamura, T. Takahashi, T. Kii, H. Ohgaki, and H. Toyokawa, Phys. Rev. C **72**, 044004 (2005).
[4] V. D. Efros, W. Leidemann, and G. Orlandini, Phys. Rev. Lett. **78**, 4015 (1997).
[5] A. F. Iyudin, O. Reimer, V. Burwitz, J. Greiner, and A. Reimer, A&A **436**, 763 (2005); L. A. Anchordoqui, J. F. Beacom, H. Goldberg, S. Palomares-Ruiz, T. J. Weiler,(2006) astro-ph/0611581; R. Diehl, private communication.
[6] V. D. Efros, W. Leidemann, and G. Orlandini, Phys. Lett. B **338**, 130 (1994).
[7] R. B. Wiringa, V. G. J. Stoks, and R. Schiavilla, Phys. Rev. C **51**, 38 (1995).
[8] R. Machleidt, Phys. Rev. C **63**, 024001 (2001).
[9] V. G. J. Stoks, R. A. M. Klomp, C. P. F. Terheggen, and J. J. de Swart, Phys. Rev. C **49**, 2950 (1994).
[10] D. R. Entem and R. Machleidt, Phys. Rev. C **68**, 041001(R) (2003).
[11] E. Epelbaum, A. Nogga, W. Glöckle, and H. Kamada, Ulf-G. Meißner, H. Witala, Phys. Rev. C **66**, 064001 (2002).
[12] S. C. Pieper, V. R. Pandharipande, R. B. Wiringa, and J. Carlson, Phys. Rev. C **64**, 014001 (2001).
[13] S. C. Pieper, K. Varga, and R. B. Wiringa, Phys. Rev. C **66**, 044310 (2002).
[14] S. C. Pieper, R. B. Wiringa, and J. Carlson, Phys. Rev. C **70**, 054325 (2004).
[15] P. Navrátil, J. P. Vary, and B. R. Barrett, Phys. Rev. Lett. **84**, 5728 (2000).
[16] P. Navrátil and E. W. Ormand, Phys. Rev. C. **68**, 034305 (2003).
[17] P. Navrátil and E. Caurier, Phys. Rev. C. **69**, 014311 (2004).
[18] W. Polyzou and W. Glöckle, Few-Body Syst. **9**, 97 (2002).
[19] P. Doleschall, I. Borbély, Z. Papp, and W. Plessas, Phys. Rev. C **67**, 064005 (2003).
[20] A. M. Shirokov, A. I. Mazur, S. A. Zaytsev, J. P. Vary, and T. A. Weber, Phys. Rev. C **70**, 044005 (2004).
[21] A. M. Shirokov, J. P. Vary, A. I. Mazur, S. A. Zaytsev, and T. A. Weber, Phys. Lett. B **621**, 96 (2005).
[22] H. Feldmeier, T. Neff, R. Roth, and J. Schnack, Nucl. Phys. **A632**, 61 (1998).
[23] T. Neff and H. Feldmeier, Nucl. Phys. **A713**, 311 (2003).
[24] R. Roth, T. Neff, H. Hergert, and H. Feldmeier, Nucl. Phys. **A745**, 3 (2004).
[25] R. Roth, P. Papakonstantinou, N. Paar, H. Hergert, T. Neff, and H. Feldmeier, Phys. Rev. C **73**, 044312 (2006).
[26] N. Paar, P. Papakonstantinou, H. Hergert, and R. Roth, Phys. Rev. C **74**, 014318 (2006).
[27] T. Neff and H. Feldmeier, Nucl. Phys. **A738**, 357 (2004).
[28] T. Neff, H. Feldmeier, and R. Roth, Nucl. Phys. **A752**, 321 (2005).
[29] R. Roth, H. Hergert, P. Papakonstantinou, T. Neff, and H. Feldmeier, Phys. Rev. C **72**, 034002 (2005).
[30] J. M. Eisenberg and W. Greiner, *Excitation mechanisms of the nucleus* (North-Holland Publishing Company, Amsterdam, 1970).
[31] H. Arenhövel and M. Sanzone, Few-Body. Syst. Suppl. **3**, 1 (1991).
[32] J. Golak, R. Skibiǹski, W. Glöckle, H. Kamada, A. Nogga, H. Witala, V. D. Efros, W. Leidemann, G. Orlandini, and E. L. Tomusiak, Nucl. Phys. **A707**, 365 (2002).
[33] V. D. Efros, W. Leidemann, and G. Orlandini, Few-Body Syst. **26**, 251 (1999).
[34] D. Andreasi, W. Leidemann, C. Reiß, and M. Schwamb, Eur. Phys. J. A **24**, 361 (2005).
[35] V. D. Efros, W. Leidemann, G. Orlandini, and E. L. Tomusiak, Phys. Lett. B **484**, 223 (2000).
[36] V. D. Efros, W. Leidemann, G. Orlandini, and E. L. Tomusiak, Phys. Rev. C **69**, 044001 (2004).
[37] V. D. Efros, W. Leidemann, G. Orlandini, and E. L. Tomusiak, Phys. Rev. C **72**, 011002(R) (2005).
[38] S. Bacca, M. A. Marchisio, N. Barnea, W. Leidemann, and G. Orlandini, Phys. Rev. Lett. **89**, 052502 (2002).
[39] S. Bacca, N. Barnea, W. Leidemann, and G. Orlandini, Phys. Rev. C. **69**, 057001 (2004).
[40] S. Bacca, H. Arenhövel, N. Barnea, W. Leidemann, and G. Orlandini, Phys. Lett. B **603**, 159 (2004).
[41] S. Quaglioni, W. Leidemann, G. Orlandini, N. Barnea, and V. D. Efros, Phys. Rev. C **69**, 044002 (2004).
[42] S. Quaglioni, V. D. Efros, W. Leidemann, and G. Orlandini, Phys. Rev. C **72**, 064002 (2005).
[43] D. Andreasi, S. Quaglioni, V. D. Efros, W. Leidemann, and G. Orlandini, Eur. Phys. J. **A27**, 47 (2006).
[44] I. Stetcu, S. Quaglioni, S. Bacca, B. R. Barrett, C. W. Johnson, P. Navratil, N. Barnea, W. Leidemann, and G. Orlandini, nucl-th/0605056.
[45] N. Barnea and A. Novoselsky, Ann. Phys. (N.Y.) **256**, 192 (1997).
[46] N. Barnea and A. Novoselsky, Phys. Rev. A **57**, 48 (1998).
[47] N. Barnea, Phys. Rev. A **59**, 1135 (1999).
[48] N. Barnea, W. Leidemann, and G. Orlandini, Phys. Rev. C **74**, 034003 (2006).
[49] A. Dellafiore and E. Lipparini, Nuc. Phys. **A388**, 639 (1982).
[50] D. Gazit, private communication.
[51] D. Gazit, N. Barnea, S. Bacca, W. Leidemann, and G. Orlandini, nucl-th/0610025.
[52] R. Ladenburg and F. Reiche, Naturwiss **11**, 873 (1923);

W. Kuhn, Z. Phys. **33**, 408 (1923); L. H. Thomas, Naturwiss **13**, 627 (1925).
[53] V. N. Fetisov, A. T. Gorbunov, and A. T. Varfolomeev, Nucl. Phys. **A71**, 305 (1965).
[54] Yu. M. Arkatov, *et al.*, Yad. Konst. **4**, 55 (1979).
[55] B. L. Berman, D. D. Faul, P. Meyer, and D. L. Olson, Phys. Rev. C **22**, 2273 (1980).
[56] G. Feldman, M. J. Balbes, L. H. Kramer, J. Z. Williams, H. R. Weller, and D. R. Tilley, Phys. Rev. C **42**, R1167 (1990).
[57] D. P. Wells, D. S. Dale, R. A. Eisenstein, F. J. Federspiel, M. A. Lucas, K. E. Mellendorf, A. M. Nathan, and A. E. O'Neill, Phys. Rev. C **46**, 449 (1992).